Nature of vortex lattice disordering at the onset of the peak effect

X. S. Ling* and J. E. Berger

Department of Physics, Brown University, Providence, Rhode Island 02912

D. E. Prober

Department of Applied Physics & Physics, Yale University, New Haven, Connecticut 06520-8284

We report a transport study of the onset of the peak effect in a $2H$-NbSe$_2$ single crystal with very weak pinning. At low driving current, we find that at the onset of the peak effect, where the resistance starts to dip with increasing field, the resistance is hysteretic upon field cycling. The resistance is higher for upward field sweeps than for downward sweeps. The difference between the two has a double-peak feature, indicative of two-stage disordering of a vortex lattice. The resistance hysteresis and the two-stage feature disappear after cold-working the sample. The onset field of the peak effect is found to depend on driving current nonmonotonically, suggesting reentrant driven disorder-order and order-disorder transitions in the peak-effect regime. [S0163-1829(98)51106-X]

Pinning of Abrikosov vortex lines by disorder makes type-II superconductors useful in carrying electrical current with minimal loss in strong magnetic fields. Thermally activated vortex creep leads to reduction in critical current,[1] significant especially in high-T_c superconductors.[2] It was thus a surprise that the critical current in very clean high-T_c superconducting YBa$_2$Cu$_3$O$_{7-\delta}$ crystals was found to *increase* sharply with increasing temperature just before it vanishes.[3] It turns out that this phenomenon, known as the *peak effect*, occurs in many low-T_c type-II superconductors.[4,5] Although rarely discussed in the textbooks of superconductivity, the pursuit of its origin led to much improved understanding of the problems of random pinning, notably the collective pinning model of Larkin-Ovchinnikov.[6,7]

Figure 1 outlines the basic phenomena in a low-T_c type-II superconductor $2H$-NbSe$_2$ (sample ''XV1-2,'' see below). As shown by the solid line in Fig. 1, when a driving current is applied (here $I = 40$ mA), and the magnetic field is increased, the resistance is zero at first and starts to increase at some field. Then, before reaching the normal-state value it suddenly dips, in this case almost to zero. Finally it increases again rapidly to the normal-state value. If a critical current is defined at a certain voltage criterion, say 1 μV, a sharp peak in critical current appears, hence the label ''peak effect,'' as shown by the open circles in Fig. 1. Since the resistance is a measure of the average vortex velocity, its increase or decrease with increasing field or temperature signals a more mobile or a more sluggish vortex lattice. At a fixed driving current or force, the sudden drop in resistance indicates a dramatic enhancement of the pinning of the vortex lattice. This behavior is believed to be related to a rapid softening of the vortex lattice since a soft lattice can easily adjust itself to the random pins.[6,7] Nevertheless, there are still open fundamental questions regarding the underlying physics of this unusual phenomenon, e.g., whether the onset of the peak effect is associated with a topological phase transition with topological defects (edge dislocations, etc.) appearing spontaneously in the vortex lattice. Resolving these issues will

deepen our understanding of the peak effect as well as the generic problem of pinned elastic phases encountered in many physical systems.

In this paper, we report striking effects of vortex dynamics observed at the onset of the peak effect in a high-quality $2H$-NbSe$_2$ single crystal with very weak pinning. Our results suggest that the onset of the peak effect is indeed associated with topological transitions, possibly of both equilibrium and dynamic origins.

In this study, a total of three $2H$-NbSe$_2$ single crystal samples are studied, all of which exhibit a peak effect. The results presented here are from the sample (''XV1-2'') which has the most pronounced peak effect (with highest ratio of I_c-maximum/I_c-minimum≈ 5). The sample dimensions are ≈ 1.38 mm$(l) \times 1.14$ mm$(w) \times 0.02$ mm(t). The sample-growth procedures have been described elsewhere.[8] Standard four-probe techniques are used for transport measurements. Slow curing silver pastes (DuPont 4929N) are used for contacts. The contacts are cured on a hot plate (≈ 40 °C) for 30
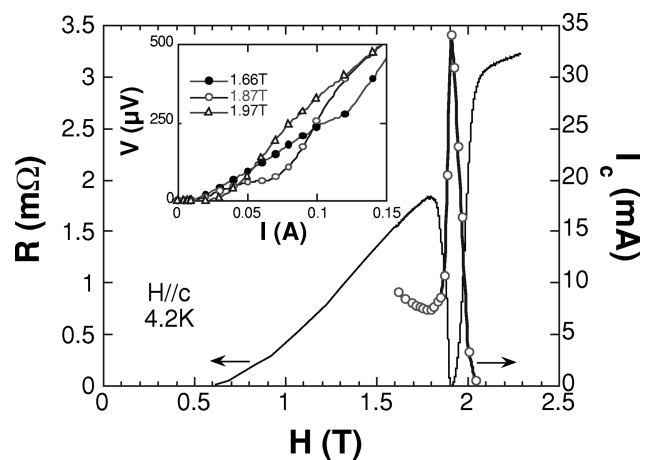

FIG. 1. Left-hand axis plots resistance as a function of magnetic field at a driving current of 40 mA. Right-hand axis plots critical current as a function of magnetic field at a voltage level of 1 μV. Inset shows *IV* curves for three different magnetic fields.
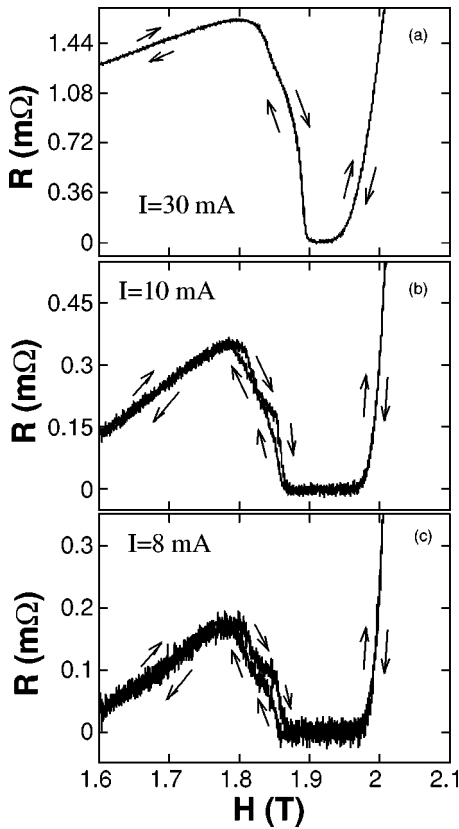
FIG. 2. Resistance as a function of magnetic field for three different driving currents: (a) $I = 30$ mA, (b) $I = 10$ mA, (c) $I = 8$ mA. Arrows indicate direction of field sweep.

FIG. 3. (a) Difference in sample resistance for upward and downward magnetic field sweeps. (b) Current dependence of ΔR for a fixed field of 1.85 T.

min with typical contact resistance less than 1 Ω. Large gold ribbons $[50 \, \mu\text{m}(w) \times 25 \, \mu\text{m}(t)]$ are used as current leads, and thin gold wires (diameter 12.5 μm) are used as voltage probes (spaced ≈ 0.5 mm apart). The important physical parameters of this sample are residual resistance ratio $R(300 \, \text{K})/R_n(7.3 \, \text{K}) = 19.1$, zero-field transition $T_c = 7.21$ K, and width $[(10-90 \, \%)R_n] = 60$ mK, all of which are indicative of good quality. For critical current measurements, as shown in Fig. 1 inset, the magnetic field is held constant while IV curves are traced, either with an XY recorder (using an analog voltmeter) or a computer (using a digital nanovoltmeter Keithley 182). The sample is immersed in a liquid helium bath. The bath pressure is carefully regulated and the bath temperature is stable to within 0.5 mK for a period of ≈ 6 h. Typically in our setup, no heating effects are measurable up to 250 mA, beyond which thermal runaway occurs. The background thermal voltage is small ($\approx 0.8 \, \mu$V) and stable (independent of sample current and field). For field-sweep measurements, a constant current is supplied (employing a high precision, HP 3245A, universal source) to the sample while the voltage is recorded as the field is slowly swept up and down at a rate of 9.2 Oe/sec. Test runs with sample current reversed are also carried out and give identical results.

Figure 2 shows the field dependence of the sample resistance for three different driving currents: 30, 10, and 8 mA. The arrows indicate the directions of the field sweeps. Several significant features should be pointed out: (1) the resistance is reversible in two field regimes, below the peak of the resistance ($H < 1.78$ T) and above the minimum of the resis-
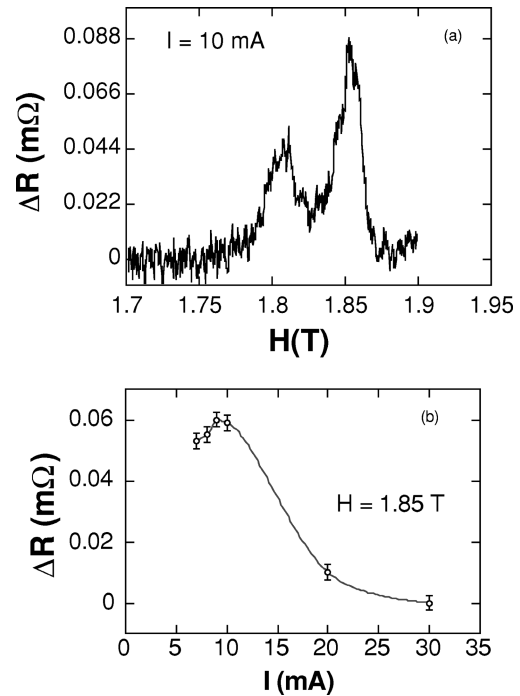
tance ($H > 1.9$ T), for all driving currents; (2) in the field regime where the resistance decreases with increasing field (from here on we shall refer to this regime as the *peak effect regime* and the resistance peak field, H_0, as the *onset of the peak effect*), the resistance is hysteretic, i.e., the resistance is higher for upward field sweeps (or field-up) than that for downward sweeps (or field-down); (3) the drop of resistance from the peak to the valley seems to involve two steps. For field-up sweeps, there are two steep jumps, while for field-down runs, only a shoulder is visible in the peak-effect regime.

For a fixed driving current and quenched disorder, the difference between the H_{up} and H_{down} resistances reflects different degrees of topological order in the vortex arrays as they are driven through the random pinning potentials. The difference between H_{up} and H_{down} resistances at 10 mA is plotted in Fig. 3(a) and gives two striking peaks. The current dependence of this difference at $H = 1.85$ T is plotted in Fig. 3(b). The absence of data points below 7 mA in Fig. 3(b) is due to the fact that at very low driving currents the signals drop below our sensitivity for fields below 1.98 T. We should also cautiously point out that, in Fig. 3(a), the drop to zero in ΔR at the high field side is due to the loss of signal in the resistance valley. The double-peak feature, however, is unquestionable.

Following these experiments, we cut a small piece (1.38 mm $\times$ 0.25 mm $\times$ 0.02 mm, sample "XV1-3") from this sample ("XV1-2") using a razor blade (the cutting causes apparent large scale disorder, visible as ripples on the surface of the sample). The new sample ("XV1-3") is then measured using the same field and current configuration. In this smaller sample, the critical current at 1.80 T is twice that of the original uncut sample although the width of the new sample is four times smaller (the critical current density is

thus eight times higher). Remarkably, the peak effect is still present in the sample, though less pronounced, I_c max/min ≈ 1.4 (≈ 5 in the uncut sample, see Fig. 1). The resistance hysteresis, however, disappears along with the shoulder feature in the peak-effect regime. Another sample with similar ratio of I_c-max/I_c-min shows behavior very similar to that of the cut sample. Clearly, the resistance hysteresis and the resistance shoulder reported here are intimately related to the weak disorder and thus the long-length-scale physics of the vortex lattice (see below).

Resistance hysteresis implies metastability in the moving vortex lattice. Hysteresis, due to much stronger pinning, of orders of magnitude larger than what is seen here, has been reported before, extending to far below the peak effect regime.[9] What is striking here is that, in this sample with very weak disorder, the resistance hysteresis appears only at the onset of the peak effect and becomes more pronounced at low driving current. The resistance hysteresis seen here is likely due to the difference in the population of topological defects in the H_{up} and H_{down} vortex states. The H_{down} state has some extra "frozen-in" defects from the high-field disordered phase, while both H_{up} and H_{down} vortex states are defective in this regime. H_{up} and H_{down} resistances merge at H_0 indicating that a stable elastic phase is present for $H < H_0$ and the vortex lattice becomes defective *spontaneously* as it enters the peak-effect regime $H > H_0$. The low-field defect-free elastic phase, dubbed the "Bragg glass,"[10] is a subject of recent theoretical interests.[10–13] The shoulder and the two-step feature in Fig. 2 suggest that the disordering of the Bragg glass phase may involve two stages, reminiscent of the KTHNY melting of two-dimensional solids.[14]

We should contrast our results with those observed[15] in high-T_c YBa$_2$Cu$_3$O$_{7-\delta}$ (YBCO) systems. There too, a resistance hysteresis appears at low driving currents, but with very different characteristics. The H_{down} (or T_{down}) resistance is higher than that of the H_{up} (or T_{up}), exactly the opposite of what is seen here. In YBCO, the hysteresis occurs at the onset of ohmic resistance where the resistance increases with increasing field or temperature.[15] Here the hysteresis appears at the onset of the peak effect where the resistance starts to drop with increasing field, while the high-field side of the peak-effect regime is completely reversible. The sharp rise of resistance with increasing H or T in YBCO was attributed to the loss of vortex-lattice rigidity, i.e., vortex-lattice melting. The drop of resistance with increasing H or T in the peak-effect regime was also interpreted as due to the loss of vortex-lattice rigidity,[6,7] or melting.[16] These seemingly contradictory interpretations may not be mutually exclusive. The two may be reconciled by considering the effects of lattice rigidity on vortex dynamics. On the one hand, the loss of the lattice rigidity allows individual vortex lines to follow the random potentials, thus enhancing pinning. On the other hand, it also promotes thermal wandering of the vortex lines between pinning sites, thereby reducing pinning. Which of the two tendencies manifests itself may depend on the details of disorder in a particular system.

From Fig. 2, one notices that the onset of the peak effect shifts slightly with increasing driving current, from $H_0 = 1.780$ T at 8 mA to 1.799 T at 30 mA. We find that in fact there is a reentrant behavior in H_0 vs driving current. Figure 4 is a plot of resistance vs field for driving currents at 9, 20,
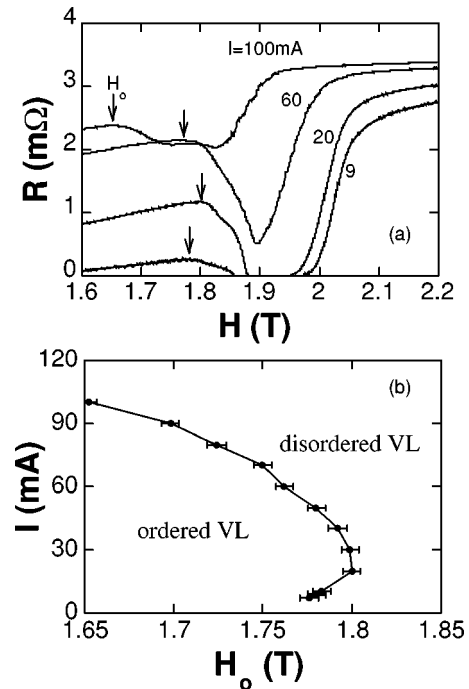

FIG. 4. (a) Resistance as a function of field for four different driving currents: 9, 20, 60, and 100 mA. Arrows indicate onset of peak effect, H_0. (b) Phase diagram.

60, and 100 mA. Only the H_{down} data are shown here. Figure 4(b) is a plot of I vs H_0. With increasing driving current, H_0 first increases slightly from 1.776 T at 7 mA to 1.800 T at 20 mA, then it starts to shift downward for $I > 40$ mA.

Since H_0 marks a transition from an ordered (more appropriately, quasiordered[10,13]) phase at $H < H_0$ to a more disordered phase at $H > H_0$, Fig. 4(b) would suggest a reentrant behavior in the moving vortex array as a function of driving current in the peak-effect regime. At $H = 1.790$ T, e.g., the moving vortex phase is disordered for $I < 14.0$ mA, ordered for 14.0 mA $< I <$ 41.5 mA, and again disordered for $I > 41.5$ mA.

The lower part of the dynamic phase diagram in Fig. 4(b) is very similar to those identified previously[17,18] using a peak in current dependent differential resistance (i.e., a peak in dV/dI vs I). We should emphasize, however, the phase diagram identified here using the onset field of the peak effect H_0 is independent of the interpretation of the shape of the IV curves. We merely use the notion[6,7] that the onset of the peak effect is a signature of vortex lattice disordering.

We also carry out an extensive study of the IV curves across the peak-effect regime for each of the samples. Three of these, for fields below, inside, and above the J_c peak, are plotted as an inset in Fig. 1. The weak pinning in our sample allows us to drive the system into the true flux-flow regime with a modest current and without heating, allowing us to explore a new dynamic regime where the vortex lattice becomes again disordered. A detailed analysis of these IV characteristics will be presented in a separate report.[19]

If the lower part of Fig. 4(b) marks a dynamic crystallization[20] of the vortex array with increasing driving current, the upper part of Fig. 4(b) would suggest that the moving vortex array undergoes yet another transition from an ordered phase to a disordered phase at a higher driving

RAPID COMMUNICATIONS

current. It should be noted that there was a brief conjecture[21] of a dynamic melting transition caused by collision with random pinning sites. Here we argue that the reentrant behavior is due to different components of the random pinning potentials. It was suggested[22] that for increasing vortex velocity the pinning effect diminishes for rare regions of strong pins while it grows for dense weak random pins. We thus interpret the lower part of Fig. 4(b) as a transition from a disordered phase to an ordered phase due to the diminishing role of rare strong pins, and the upper part of Fig. 4(b) as a transition from an ordered phase to a disordered phase due to the increasing effect of the dense random weak pins. To the best of our knowledge, this is the first experimental evidence that a moving vortex lattice is unstable at high velocities in the presence of random pins. This result may be relevant to other systems such as sliding friction,[23] sedimenting colloidal crystals,[24] etc., where the stability of a moving lattice against random forces is also important.

In summary, we have carried out a detailed study of the onset of the peak effect in a $2H$-NbSe$_2$ crystal with very weak pinning. We find that (1) a resistance hysteresis appears at low driving current and occurs only at the onset of the peak effect, suggesting a stable elastic phase (Bragg glass) at low fields and the spontaneous nature of the vortex lattice disordering; (2) the transition between the Bragg glass phase and disordered phase seems to involve two stages; (3) the driven-ordered dynamic vortex phase is unstable at high velocity leading to reentrant dynamic transitions in the peak-effect regime. It will be very interesting to see whether the effects seen here in $2H$-NbSe$_2$ also appear in the peak-effect regime in high-T_c YBa$_2$Cu$_3$O$_{7-\delta}$ crystals.

Note added. Recently, we received an unpublished paper[25] in which the ac susceptibility measurements on $2H$-NbSe$_2$ crystals revealed two discontinuous transitions in the peak-effect regime when the sample is cooled in zero field.

*Corresponding author. Electronic address: xsling@brown.edu.

[1] P. W. Anderson, Phys. Rev. Lett. **9**, 309 (1962).

[2] Y. Yeshurun and A. P. Malozemoff, Phys. Rev. Lett. **60**, 2202 (1988); M. Tinkham, *ibid.* **61**, 1658 (1988).

[3] X. S. Ling and J. I. Budnick, in *Magnetic Susceptibility of Superconductors and Other Spin Systems*, edited by R. A. Hein *et al.* (Plenum Press, New York, 1991), p. 377; G. D'Anna *et al.*, Europhys. Lett. **25**, 225 (1994); M. Ziese *et al.*, Phys. Rev. B **50**, 9491 (1994); W. K. Kwok *et al.*, Phys. Rev. Lett. **73**, 2614 (1994); X. S. Ling, J. I. Budnick, and B. W. Veal, Physica C **282**, 2191 (1997).

[4] S. H. Autler, E. S. Rosenblum, and K. Gooen, Phys. Rev. Lett. **9**, 489 (1962); W. DeSorbo, Rev. Mod. Phys. **36**, 90 (1964).

[5] P. H. Kes and C. C. Tsuei, Phys. Rev. B **28**, 5126 (1983); P. Koorevaar *et al.*, *ibid.* **42**, 1004 (1990); M. Higgins and S. Bhattacharya, Physica C **257**, 233 (1996), and references therein.

[6] A. B. Pippard, Philos. Mag. **19**, 217 (1969).

[7] A. I. Larkin and Yu. N. Ovchinnikov, J. Low Temp. Phys. **34**, 409 (1979).

[8] B. J. Dalrymple, S. Mroczkowski, and D. E. Prober, J. Cryst. Growth **74**, 575 (1986).

[9] M. Steingart, A. Putz, and E. Kramer, J. Appl. Phys. **44**, 5580 (1973); R. Wördenweber, P. H. Kes, and C. C. Tsuei, Phys. Rev. B **33**, 3172 (1986); W. Henderson, E. Y. Andrei, M. J. Higgins, and S. Bhattacharya, Phys. Rev. Lett. **77**, 2077 (1996).

[10] T. Nattermann, Phys. Rev. Lett. **64**, 2454 (1990); T. Giamarchi and P. Le Doussal, *ibid.* **72**, 1530 (1994); J. Kierfeld, T. Nattermann, and T. Hwa, Phys. Rev. B **55**, 626 (1997).

[11] M. J. P. Gingras and D. A. Huse, Phys. Rev. B **53**, 15 193 (1996).

[12] D. S. Fisher, Phys. Rev. Lett. **78**, 1964 (1997).

[13] T. Giamarchi and P. Le Doussal, Phys. Rev. Lett. **76**, 3408 (1996); S. Ryu, M. Hellerqvist, S. Doniach, A. Kapitulnik, and D. Stroud, *ibid.* **77**, 5114 (1996); L. Balents, M. C. Marchetti, and L. Radzihovsky, *ibid.* **78**, 751 (1997); K. Moon, R. T. Scalettar, and G. T. Zimanyi, *ibid.* **77**, 2778 (1996).

[14] J. M. Kosterlitz and D. J. Thouless, J. Phys. C **6**, 1181 (1973); B. I. Halperin and D. R. Nelson, Phys. Rev. Lett. **41**, 121 (1978); A. P. Young, Phys. Rev. B **19**, 1855 (1979).

[15] H. Safar *et al.*, Phys. Rev. Lett. **69**, 824 (1992); M. Charalambous *et al.*, *ibid.* **71**, 436 (1993); W. K. Kwok *et al.*, *ibid.* **72**, 1092 (1994); W. Jiang *et al.*, *ibid.* **74**, 1438 (1995).

[16] C. Tang, X. S. Ling, S. Bhattacharya, and P. M. Chaikin, Europhys. Lett. **35**, 597 (1996).

[17] S. Bhattacharya and M. J. Higgins, Phys. Rev. Lett. **70**, 2617 (1993); Phys. Rev. B **49**, 10 005 (1994).

[18] M. C. Hellerqvist, D. Ephron, W. R. White, M. R. Beasley, and A. Kapitulnik, Phys. Rev. Lett. **77**, 5114 (1996).

[19] J. E. Berger, X. S. Ling, and D. E. Prober (unpublished).

[20] A. E. Koshelev and V. M. Vinokur, Phys. Rev. Lett. **73**, 3580 (1994).

[21] T. K. Worthington *et al.*, Phys. Rev. B **46**, 11 854 (1992).

[22] A. I. Larkin and Yu. N. Ovchinnikov, Sov. Phys. JETP **53**, 1221 (1981).

[23] See *Physics of Sliding Friction*, edited by B. N. J. Persson and E. Tosatti (Kluwer Academic, Dordrecht, 1996).

[24] R. Lahiri and S. Ramaswamy, Phys. Rev. Lett. **79**, 1150 (1997).

[25] S. Banerjee *et al.* cond-mat/9708149 (unpublished).